Magnetic flux loop in high-energy heavy-ion collisions

Adrian Dumitru[a,b,c], Yasushi Nara[d] and Elena Petreska[b,c]
[a] RIKEN BNL Research Center,
Brookhaven National Laboratory, Upton, NY 11973, USA
[b] Department of Natural Sciences,
Baruch College, CUNY, 17 Lexington Avenue,
New York, NY 10010, USA
[c] The Graduate School and University Center,
The City University of New York,
365 Fifth Avenue, New York, NY 10016, USA
[d] Akita International University,
Yuwa, Akita-city 010-1292, Japan

We consider the expectation value of a chromo-magnetic flux loop in the immediate forward light cone of collisions of heavy nuclei at high energies. Such collisions are characterized by a non-linear scale Q_s where color fields become strong. We find that loops of area greater than $\sim 2/Q_s^2$ exhibit area law behavior, which determines the scale of elementary flux excitations ("vortices"). We also estimate the magnetic string tension, $\sigma_M \simeq 0.12\, Q_s^2$. By the time $t \sim 1/Q_s$ even small loops satisfy an area law while substantial magnetic fields remain only at large distances. We describe corrections to the propagator of semi-hard gluons at very early times in the background of fluctuating magnetic fields.

Collisions of heavy ions at high energies provide opportunity to study non-linear dynamics of strong QCD color fields [1]. The field of a very dense system of color charges at rapidities far from the source is determined by the classical Yang-Mills equations with a recoilless current along the light cone [2]. It consists of gluons characterized by a transverse momentum p_T on the order of the density of valence charges per unit transverse area Q_s^2 [3]; this *saturation momentum* scale separates the regime of non-linear color field interactions at $p_T \lesssim Q_s$ or distances $r \gtrsim 1/Q_s$ from the perturbative regime at $p_T \gg Q_s$. Near the center of a large nucleus this scale is expected to exceed $\sim$ 1.5 GeV at BNL-RHIC or CERN-LHC collider energies, for a probe in the adjoint representation of the color gauge group. The classical field solution provides the leading contribution to an expansion in terms of the coupling and of the inverse saturation momentum.

The soft field produced in a collision of two nuclei is then a solution of the Yang-Mills equations satisfying appropriate matching conditions on the light cone [4]. Most interestingly, right after the impact strong longitudinal chromo-magnetic fields $B_z \sim 1/g$ develop due to the fact that the individual projectile and target fields do not commute [5, 6]. They fluctuate randomly according to the random local color charge densities of the valence sources. In this Letter we show that magnetic loops W_M exhibit area law behavior, and we compute the magnetic string tension. We also determine W_M for finite times after the collision from a numerical solution of the Yang-Mills equations. Finally, we sketch how the background of magnetic fields affects propagation of semi-hard particles with transverse momenta somewhat above Q_s.

We consider a spatial Wilson loop with radius R in the plane transverse to the beams,

$$\begin{aligned} M(R) &= \mathcal{P}\exp\left(ig\int\limits_{-\pi}^{\pi} d\theta\, \frac{\partial x^i}{\partial\theta} A^i\right) \\ W_M(R) &= \frac{1}{N_c}\left\langle \mathrm{tr}\, M(R)\right\rangle \ , \end{aligned} \tag{1}$$

where $x = R(\cos\theta, \sin\theta)$, and path ordering is with respect to the angle θ; in numerical lattice simulations it is more convenient to employ a square loop. We compare, also, to the expectation value of the Z(N_c) part of the loop; for a magnetic field configuration corresponding simply to a superposition of independent vortices the loop should equal $\exp(2\pi i\, n/N_c)$, with n the total vortex charge piercing the loop. Thus, for two colors we compute

$$W_M^{Z(2)}(R) = \langle \mathrm{sgn}\, \mathrm{tr}\, M(R)\rangle \tag{2}$$

where sgn() denotes the sign function. Comparing (1) to (2) tests the interpretation that the drop-off of $W_M(R)$ is due to Z(N_c) vortices, without requiring gauge fixing of the SU(N_c) links [7].

The field in the forward light cone immediately after a collision [4], at proper time $\tau \equiv \sqrt{t^2 - z^2} \to +0$, is given by $A^i = \alpha_1^i + \alpha_2^i$. In turn, before the collision the individual fields of projectile and target are 2d pure gauges,

$$\alpha_m^i = \frac{i}{g}\, U_m\, \partial^i U_m^\dagger \quad , \quad \partial^i \alpha_m^i = g\rho_m \ , \tag{3}$$

where $m = 1$, 2 labels projectile and target, respectively, and U_m are SU(N) gauge fields. Eqs. (3) can be solved

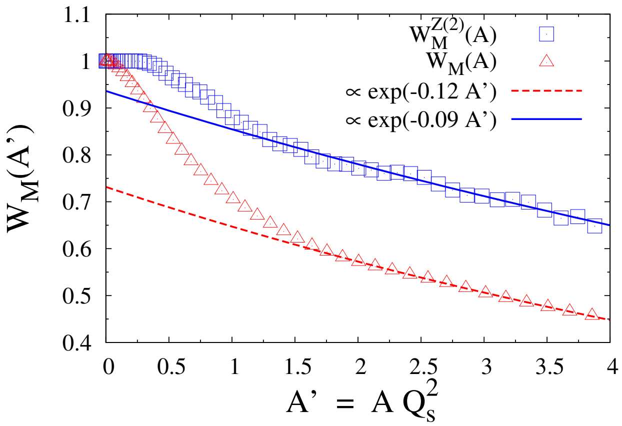

FIG. 1: Expectation value of the magnetic flux loop right after a collision of two nuclei (time $\tau = +0$) as a function of its area $A' \equiv A\,Q_s^2$. We define $Q_s^2 = (C_F/2\pi)\,g^4\mu^2$. Symbols show numerical results for $SU(2)$ Yang-Mills on a 4096^2 lattice; the lattice spacing is set by $g^2\mu_L = 0.0661$. The lines represent fits over the range $4 \geq A' \geq 2$.

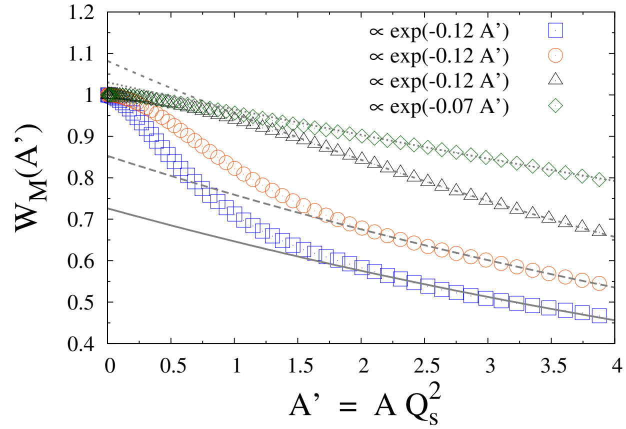

FIG. 2: Time evolution of the magnetic flux loop after a collision of two nuclei (4096^2 lattice, $g^2\mu_L = 0.05$). From bottom to top, the curves correspond to time $\tau \times g^2\mu = 0$, 1, 2, 3, where $g^2\mu \simeq 3Q_s$ so that $\tau = 3/(g^2\mu)$ corresponds to about $\tau \simeq 1/Q_s$ in physical units.

either analytically in an expansion in the field strength [4] or numerically on a lattice [8].

The large-x valence charge density ρ is a random variable[12]. For a large nucleus, the effective action describing color charge fluctuations is quadratic,

$$S_{\rm eff}[\rho^a] = \frac{\rho^a(\mathbf{x})\rho^a(\mathbf{x})}{2\mu^2} \quad , \quad \langle\rho^a(\mathbf{x})\,\rho^b(\mathbf{y})\rangle = \mu^2\delta^{ab}\delta(\mathbf{x}-\mathbf{y})\,, \tag{4}$$

with μ^2 proportional to the thickness of a given nucleus [2]. The variance of color charge fluctuations determines the saturation scale $Q_s^2 \sim g^4\mu^2$ [3]. The coarse-grained effective action (4) applies to (transverse) area elements containing a large number of large-x "valence" charges, $\Delta A_\perp\,\mu^2 \sim \Delta A_\perp\,Q_s^2/g^4 \gg 1$.

In fig. 1 we show numerical results for W_M immediately after a collision. It exhibits area law behavior for loops larger than $A \gtrsim 2/Q_s^2$. The corresponding "magnetic string tension" is $\sigma_M/Q_s^2 = 0.12(1)$. The area law indicates uncorrelated magnetic flux fluctuations through the Wilson loop and that the area of magnetic vortices is rather small, their radius being on the order of $R_{\rm vtx} \sim 0.8/Q_s$. We do not observe a breakdown of the area law up to $A \sim 4/Q_s^2$, implying that vortex correlations are small at such distance scales. Also, restricting to the Z(2) part reduces the magnetic flux through small loops but σ_M is comparable to the full SU(2) result, if somewhat smaller.

The numerically small vortex size that we find is *parametrically* consistent with the classical Gaussian approximation at weak coupling which, as already mentioned above, applies for areas $\Delta A_\perp \gg g^4/Q_s^2$. Corrections to $S_{\rm eff}$ of higher order in ρ [9] as well as due to quantum fluctuations [10] of the fields should be investigated in the future.

Since the field of a single nucleus is a pure gauge it follows that $W_M^{\rm sngl} = 1$. Thus, if W_M is computed perturbatively one has to subtract disconnected contributions. We estimate the connected contribution to W_M after a collision of two nuclei by expanding W_M to fourth order:

$$W_M(\alpha_1^i + \alpha_2^i) - W_M^{\rm sngl}(\alpha_1^i)\,W_M^{\rm sngl}(\alpha_2^i) \;= \frac{\pi^2}{3}\frac{2N_c^2-3}{N_c^2-1}\,A^2Q_{s1}^2Q_{s2}^2\,. \tag{5}$$

This result does not require an IR cutoff. There is no contribution at order $\sim A$, hence no area law behavior and no vortices, even though there is, of course, a non-zero longitudinal magnetic field even at the "naive" perturbative level:

$$\frac{g^2}{N_c}\langle{\rm tr}\,B_z(\mathbf{r})\,B_z(\mathbf{r}')\rangle = 4\frac{N_c^2}{N_c^2-1}\,Q_{s1}^2Q_{s2}^2\log^2\frac{1}{|\mathbf{r}-\mathbf{r}'|\,\Lambda}\,. \tag{6}$$

The failure in eq. (5) to reproduce the area law behavior of W_M is related to the perturbative expansion of the Wilson loop and the interchanged integrations over the loop and over the Gaussian charge density fluctuations (4). In contrast, for the exact lattice result we compute W_M for every individual configuration of sources $\rho_{1,2}^a(x_\perp)$ and average it *a posteriori*. Any such particular configuration contains higher (magnetic) multipoles which are eliminated by a "naive" Gaussian approximation; this has been discussed in detail in the recent literature [11] which has focused on higher multipoles of electric Wilson lines, however. The area squared behavior predicted by the naive Gaussian approximation (5,6) might be visible in numerical measurements of much larger loops where the dipole moment should be dominant.

In fig. 2 we show the time evolution of the magnetic flux loop after a collision. The magnetic field strength decreases due to longitudinal expansion and so W_M approaches unity. On the other hand, the onset of area law behavior is pushed to smaller loops, implying that the size of elementary flux excitations or "vortices" decreases; by the time $\tau \sim 1/Q_s$ area law behavior is satisfied even for rather small loops. Since long wavelength magnetic fields remain even at times $\sim 1/Q_s$, it will be important in the future to understand the transition of W_M to behavior expected in *thermal* QCD.

We have also investigated the dependence of the magnetic flux loop in the adjoint representation on its area,

$$W_M^{\mathrm{adj}} = \frac{1}{N_c^2 - 1} \left\langle |\mathrm{tr}\, M|^2 - 1 \right\rangle \ , \tag{7}$$

and found behavior similar to fig. 2. The adjoint magnetic string tension is about two times larger, as expected from (7).

The third color component of the longitudinal magnetic field is shown in fig. 3. Domain-like structures where the magnetic field is either positive or negative are clearly visible; they lead to the above-mentioned area law of the Wilson loop. Also, one can see that in time the magnetic fields become weaker and smoother.

The magnetic fields modify the propagation of semi-hard modes with p_T not too far above Q_s. Quantum mechanically, the transition amplitude from a state $|x_i, t_i\rangle$ to $|x_f, t_f\rangle$ is given by a Feynman sum over paths,

$$\int_0^\infty ds \int \mathcal{D}x^\mu \left\langle \exp\, i \int\limits_0^s d\tau \left(m\dot{x}^2 + gA_\mu \dot{x}^\mu \right) \right\rangle \sim$$
$$\int_0^\infty ds \int \mathcal{D}x^\mu \exp \left(i \int\limits_0^s d\tau\, m\dot{x}^2 \right) \exp(-\sigma_M A) \ , \tag{8}$$

where $x^\mu(\tau)$ is a parametrization of the path with the given boundary conditions and length s; and $\dot{x}^\mu = dx^\mu/d\tau$. Here, the area A is that enclosed by a quantum mechanical path from the initial to the final point returning to $\mathbf{x}_i$ via the classical path; see fig. 4. The classical path is obtained by extremizing the action but a single path is a set of measure zero. Semi-classical paths can dominate the integral only if there is constructive interference among neighboring paths from within a de Broglie distance. On the other hand, destructive interference of such paths leads to Anderson localization of the wave function.

Hence, up to a numerical factor, the area in eq. (8) should be given by $A \sim s/p_T$. Integrating over the Schwinger parameter then leads to the propagator

$$\frac{i}{p^2 + i\sigma_M \frac{m}{p_T}} \ , \tag{9}$$

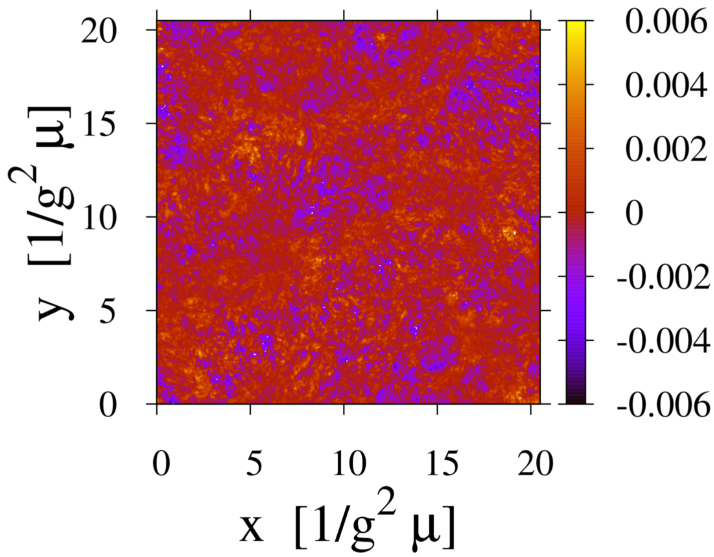

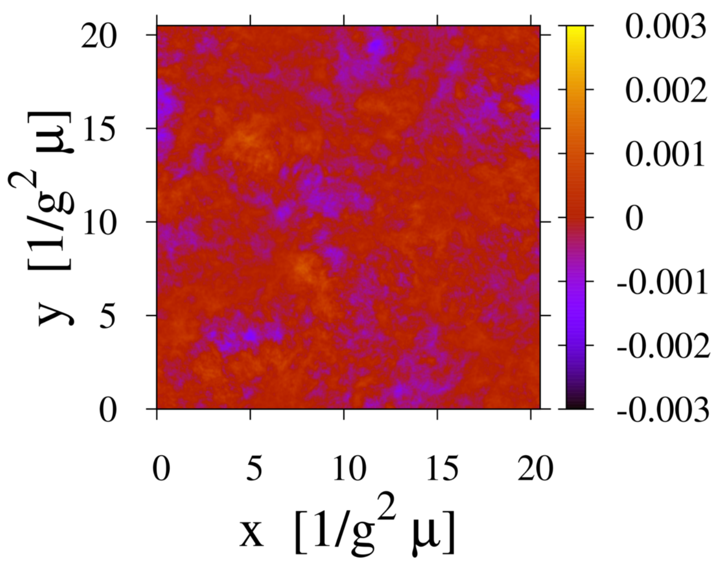

FIG. 3: Color-3 component of the magnetic field $F^3_{xy}(x, y)$ in the transverse plane at time $\tau = +0$ (top) and $1/g^2\mu \sim 1/3Q_s$ (bottom) for a single configuration of color charge sources ρ.

where $\sigma_M = 0.12\, Q_s^2$ from above and m is the mass (time-like virtuality) of the particle. This expression accounts for corrections to free propagation and could be useful for studies of the dynamics of the very early stage of a heavy-ion collision.

We obtain a rather interesting picture of the very early stage of ultrarelativistic heavy-ion collisions. Magnetic Wilson loops of area $\gtrsim 2/Q_s^2$ exhibit area law behavior

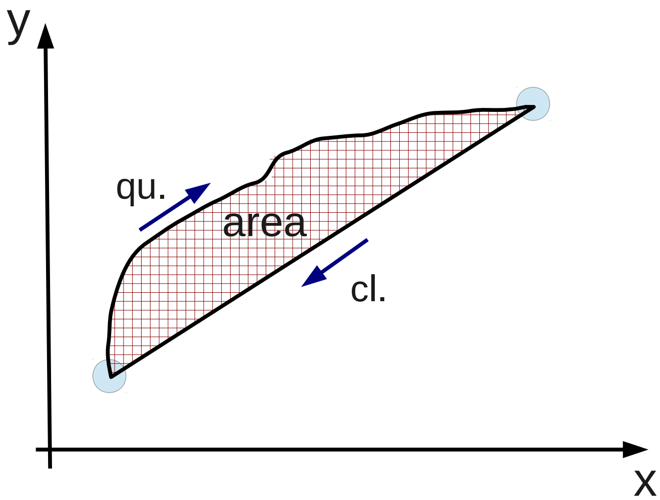

FIG. 4: Area enclosed by a quantum mechanical path shifted by about one de Broglie wavelength from the extremal classical path.

which implies uncorrelated magnetic vortex-like flux beyond the scale $R_{\rm vtx} \sim 0.8/Q_s$. This indicates that many more multipole moments rather than just the dipole are present. The vortex structure of the longitudinal magnetic field modifies propagation of particle-like modes with de Broglie wavelength somewhat larger than Q_s.

We thank A. Kovner, L. McLerran, P. Orland and R. Pisarski for helpful comments. A.D. and E.P. gratefully acknowledge support by the DOE Office of Nuclear Physics through Grant No. DE-FG02-09ER41620; and from The City University of New York through the PSC-CUNY Research Award Program, grant 65041-0043.

[1] A. H. Mueller, Nucl. Phys. B **558**, 285 (1999).
[2] L. D. McLerran and R. Venugopalan, Phys. Rev. **D 49**, 2233 (1994), Phys. Rev. **D 49**, 3352 (1994); Y. V. Kovchegov, Phys. Rev. **D 54**, 5463 (1996).
[3] J. Jalilian-Marian, A. Kovner, L. D. McLerran and H. Weigert, Phys. Rev. D **55**, 5414 (1997).
[4] A. Kovner, L. D. McLerran and H. Weigert, Phys. Rev. D **52**, 6231 (1995); Phys. Rev. D **52**, 3809 (1995).
[5] R. J. Fries, J. I. Kapusta and Y. Li, nucl-th/0604054.
[6] T. Lappi and L. McLerran, Nucl. Phys. A **772**, 200 (2006).
[7] J. D. Stack, W. W. Tucker and A. Hart, hep-lat/0011057.
[8] A. Krasnitz, Y. Nara and R. Venugopalan, Phys. Rev. Lett. **87**, 192302 (2001); T. Lappi, Phys. Rev. C **67**, 054903 (2003); Eur. Phys. J. C **55**, 285 (2008).
[9] A. Dumitru and E. Petreska, Nucl. Phys. A **879**, 59 (2012); A. Dumitru, J. Jalilian-Marian and E. Petreska, Phys. Rev. D **84**, 014018 (2011).
[10] J. Berges and S. Schlichting, arXiv:1209.0817 [hep-ph].
[11] A. Kovner and M. Lublinsky, Phys. Rev. D **83**, 034017 (2011); F. Dominguez, C. Marquet, B.-W. Xiao and F. Yuan, Phys. Rev. D **83**, 105005 (2011); A. Kovner and M. Lublinsky, arXiv:1211.1928 [hep-ph].
[12] In the context of large vs. small x this variable denotes the light-cone momentum of a parton relative to the beam hadron and should not be confused with a transverse coordinate.